Interfacial Evaluation and Microfailure Mechanisms of Carbon Fiber/Bismaleimide (BMI) Composites using Tensile/Compressive Fragmentation Tests and Acoustic Emission

Kim, Jin-Won*, Park, Joung-Man*,† and Yoon, Dong-Jin**

인장/압축 Fragmentation 시험법과 음향방출을 이용한 Carbon Fiber/Bismaleimide (BMI) Composites 의 계면 평가와 미세파괴 메커니즘 연구

김진원* · 박종만*,† · 윤동진**

KEY WORDS: Bismaleimide (BMI), Interfacial Shear Strength (IFSS), Dual Matrix Composites, Tensile/Compressive test, Acoustic Emission (AE)

ABSTRACT

Interfacial and microfailure properties of carbon fiber/bismaleimide (BMI) composites were evaluated using both tensile fragmentation and compressive Broutman tests with acoustic emission (AE). Since BMI is rather difficult matrix to apply for the conventional fragmentation test because of its too low elongation and too brittle and high modulus properties, dual matrix composite system was applied. After carbon fiber/BMI composite was prepared for rod shape by controlling differing curing stage, composites rod was embedded in toughened epoxy as outer matrix. The typical microfailure modes including fiber break, matrix cracking, and interlayer failure were observed during tensile testing, whereas the diagonal slippage in fiber ends was observed during compressive test. On the other hand, AE amplitudes of BMI matrix fracture were higher than carbon fiber fracture under tensile test because BMI matrix has very brittle and high modulus. The waveform of signals coming from BMI matrix fractures was consistent with AE amplitude result under tensile tests.

Nomenclature

τ_t , τ_c : Interfacial Shear Strength (IFSS) under Tensile and Compressive loading
σ_{fu} , σ_{fc} : Tensile and Compressive Strength of Fiber
l_c : Critical Fragment Length
l_i : Initial Fragment Length
d : Fiber Diameter
x : Matrix Crack spacing
σ_{mu} : The Stress at Which The Crack Begin to Form
V_m, V_f : The Volume Fraction of Matrix and Fiber

* Department of Polymer Science & Engineering, Research Center for Aircraft Parts Technology, Gyeongsang National University
** Nondestructive Evaluation Group, Korea Research Institute of Standards and Science

1. INTRODUTION

Bismaleimide is high-temperature polymer currently being considered for applications in elevated temperature operations for which conventional epoxy may not be sufficiently stable. They typically possess excellent thermal stability and high modulus. Bismaleimide has the advantages of better process flexibility because it can be used as a liquid-based resin or as a prepregs material. The main disadvantage has been the relatively brittle properties of the pure resin.

Interfacial properties of the carbon fiber/BMI matrix composites were evaluated using both the tensile and compressive tests with an aid of AE. The commonly used tensile fragmentation test was interested in characterizing the fiber/matrix interfacial property under axial tensile load [1]. Since BMI resin is rather difficult matrix to apply for the conventional fragmentation test due to its too brittle and high modulus properties, it can modify fragmentation test so called dual matrix composite [2,3]

Interfacial properties of the fiber/matrix were obtained by the single-fiber Broutman test to investigate the interface debonding and buckling behavior while subjecting to a transverse tensile stress [4-6]. Interfacial shear strength (IFSS) can be improved by electrodeposition (ED). [7] During tensile/compressive testing, AE test monitored the fracture signals of microfailure sources simultaneously, and correlated with IFSS [6].

2. EXPERIMENTAL

2. 1. Materials

Three types, carbon, SiC, and glass fibers were used. Carbon fiber of 7.9 ㎛ (TZ-307, Tae Kwang Co.), 14.7 ㎛ SiC (Nicalon, Nippon Carbon Co. Ltd.), and 30.3 ㎛ glass fiber (E-glass, Dow Corning Co.) were used for comparing the differing fiber failure modes. Two thermosetting resins were used, brittle BMI (Matrimide 5294, Giba-Gagy) and ductile Epoxy (YD-128, Kukdo Chemical Co.) as an outer matrix. The BMI resin system was the mixture of 4, 4'-bismaleimidodiphenylmethane (BMPM) and *O*, *O*'-diallyl bisphenol A (DABPA) in 100:85 weight ratio. Epoxy resin based on diglycidyl ether of bisphenol-A (DGEBA) was only used to holding matrix to CF/BMI composites rod. Polyoxypropylene diamine (Jeffamine D400, D2000) was used as curing agents to provide optimum condition.

2. 2. Methodologies

2. 2. 1. Preparation of Microspecimens: After the carbon fibers were fixed and poured BMI resin into a steel plate, carbon fiber/BMI composites were cured in the autoclave. Tensile and Compressive Broutman microspecimens were made of carbon fiber/BMI composite rod embedded in epoxy matrix in silicone mould as shown in figure 1.

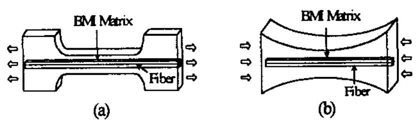

Fig. 1. Schematic illustrations showing for (a) tensile; and (b) compressive Broutman specimens

2. 2. 2. Curing Stage of BMI Resin: After mixing BMI resin at 130 ℃, 3 curing stages were divided to observe differing failure modes of BMI composites in table 1.

Table 1. The curing stage of BMI resin.

Stage	180℃	200℃	250℃
1	1 hr	-	-
2	1 hr	5 hrs	-
3	1 hr	2 hrs	5 hrs

2. 2. 3. IFSS Measurement: The fragmentation test was performed to obtain IFSS using a hand-made UTM. Ultimate fragment lengths were measured, and subsequent failure process was observed via a polarized-light microscope. When the fiber reinforced brittle matrix was stressed in tension parallel to the fiber length, multiple fracture of the matrix occurs when the fibers have the elongation to failure, and where the fibers are able to withstand the additional stress thrown onto them when the matrix fails. If there are IFSS, τ, matrix crack spacing, x, a simple calculation shows that x is given by the expression [3]

$$x = \frac{V_m \sigma_{mu} d}{2 V_f \tau} \qquad (1)$$

where V_m and V_f are the volume fraction of the matrix and fiber, respectively, d is the fiber diameter and σ_{mu} is the stress at which the cracks begin to form.

The relationship among fiber tensile strength σ_f, aspect ratio l_c/d, and conventional tensile IFSS, τ_c, was given by Kelly-Tyson [6] equation and Weibull statistics

$$\tau_t = \frac{\sigma_{fu} \cdot d}{2 l_c} \qquad (2)$$

where σ_{fu} is the tensile strength of the fiber at average critical fragment length l_c. The compressive stress on a fiber can be transferred perfectly across the break from one the fiber fragment to the other due to the fact that the fragments are still in contact with each other. A critical fragment length, as defined by the tensile load transfer model, does not exist in compressive system. According to the compressive profile, compressive IFSS, τ_c, based also on the force balance,

$$\tau_c = \frac{\sigma_{fc} \cdot d}{2 l_c} \qquad (3)$$

where critical length l_c is the original length of the fiber ($l_c = l_1$). σ_{fc} is the fiber stress at the point where the interfacial stress is insufficient to induce further fragmentation.

2. 2. 4. AE Measurement: Figure 2 shows diagram of AE and micro-specimen for tensile/compressive tests. AE sensor was attached in the center of the specimen using a couplant. AE signals were detected using a wide band sensor (Broadband Type model, WD by PAC) with peak sensitivity of 55 Ref V/(m/s) [-62.5 Ref V/mbar] and resonant frequency at 125 [650] kHz. The sensor output was amplified by 40 dB at preamplifier and passed through a band-pass filter with a range of 100 to 1200 kHz. The threshold level was set to 35 dB. Using in-built software AE waveforms and their fast *Fourier* transform (FFT) were analyzed.

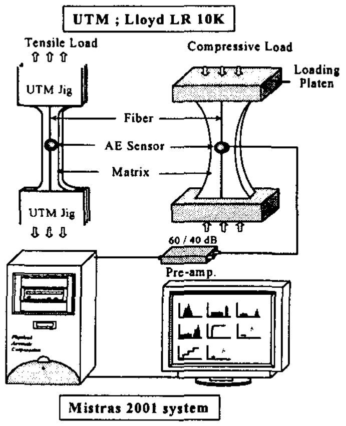

Fig. 2. Schematic diagram of instrumentation for AE

3. RESULTS and DISCUSSION

3. 1. Microfailure Modes of BMI Composites

3. 1. 1. BMI Composite by Loading Types: Figure 3 and 4 show schematic illustration and photographs of the failure modes under tensile and compressive loading in carbon fiber/BMI composites. In case of tensile test, failure modes exhibited the fracture of carbon and BMI matrix, whereas only failure modes of carbon fiber occurred in compressive test. It may because of the BMI matrix brittleness, low tensile strain and high modulus. In compressive test, the fracture of BMI matrix does not occur because of highly compressive modulus and failure stress.

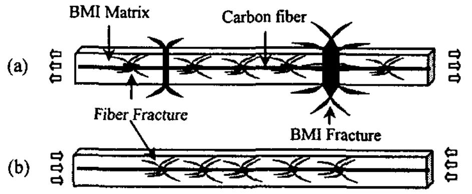

Fig. 3. Schematic illustration of microfailure modes in BMI Composite under: (a) tensile, (b) compressive load.

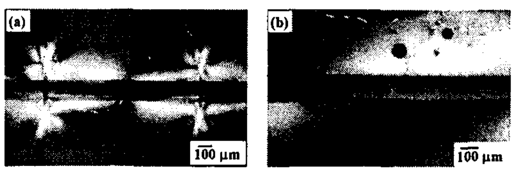

Fig. 4. Polarized-light photographs of the failure modes for BMI composites under: (a) tensile, (b) compressive

3.1.2. BMI Composites by Curing Stage: Figure 5 shows failure mode of BMI composites depending on the curing 2- and 3-stage under tensile and compressive tests. In figure 5(a) and (b), fracture of BMI matrix under tensile test occurred with several vertical cracks, plus just rough triangle shape at 2-stage, whereas a diamond shape failure was observed at 3-stage. During the following curing stages, BMI matrix crack spacing increased. In figure 5(c) and (c) carbon fiber fracture under compressive test occurred with the diagonal slippage in fiber ends. At 2-stage, overlapped diagonal slippage occurred at fracture fiber ends, whereas the slippage of fracture part occurred rather dully at 3-stage. A perfect curing at 2-stage did not occur, and a complete cure condition might occur at 3-stage.

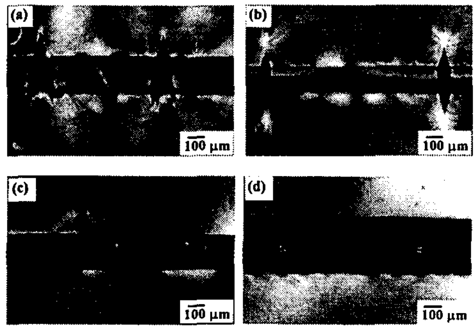

Fig. 5. Polarized-light photographs of failure modes for CF/BMI composites at differing curing stages: (a) 2- and (b) 3 stage under tensile test; (c) 2- and (d) 3-stage under compressive test.

3. 2. Evaluation of IFSS

Table 2 shows the interfacial properties of fragment length and IFSS. Figure 5 shows tensile/compressive IFSS of carbon fiber/BMI composites for 2- and 3-stages

Table 2. Interfacial Properties of BMI Composites.

Stage	Fiber	$x^{1)}$ (µm)	Tensile $l_c/d^{2)}$	Tensile τ_t	Compressive $l_c/d^{1)}$	Compressive τ_c
2	CF	1174	70.1	37.4	101.2	1.2
	SiC	1425	-[3)]	-	-	-
	GF	1106	-	-	-	-
3	CF	2748	60.8	44.7	70.1	1.4
	SiC	2325	-	-	-	-
	GF	1688	-	-	-	-

1) Matrix crack spacing
2) Aspect ratio
3) Can not measured

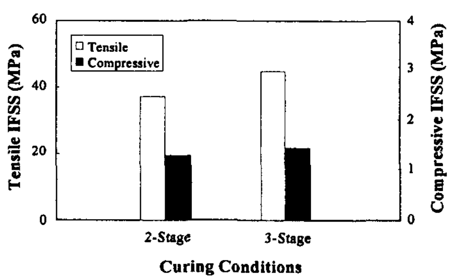

Fig. 6. IFSS of CF/BMI/Epoxy with 2 Curing Stages.

The IFSS at 3-stage appeared larger than the case at 2-stage under tensile and compressive tests. In case of SiC fiber and glass fiber, fiber breaks did not occur because break strain of fibers was similar with failure strain of BMI matrix, and only crack spacing of BMI matrix was compared with interfacial adhesion. As progressing from 2-stage to 3-stage, matrix crack spacing increased. It was considered because interfacial adhesion between the fiber and matrix increased due to perfect curing at higher temperature.

3. 3. Analysis of Acoustic Emission (AE)

Figure 7 shows the AE amplitude for carbon, SiC and glass fiber/BMI/Epoxy composites under following curing stages with stress-strain curve using tensile/compressive test. The fiber fracture and BMI matrix fracture are separated well in tensile tests for the BMI composites, whereas in compressive test AE amplitudes were rather closely separated and fracture signal from BMI matrix were not detected. At 2-stage, interfacial failure signal of fiber/BMI matrix occurred frequently, whereas fiber and matrix fracture signals were detected and interfacial failure signal did not appeared at 3-stage. It is probably because of differing curing degree between 2- and 3-stages.

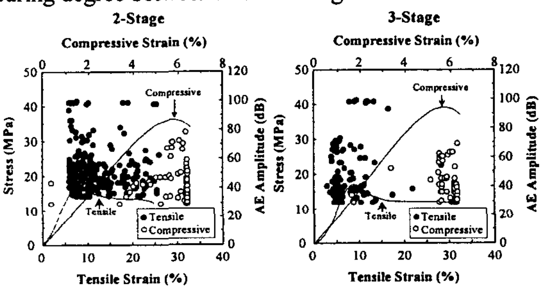

(a) CF/BMI/Epoxy Composite

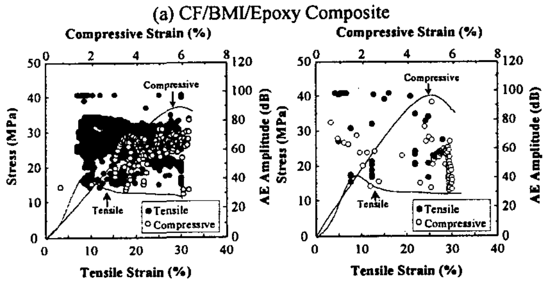

(b) SiC/BMI/Epoxy Composite

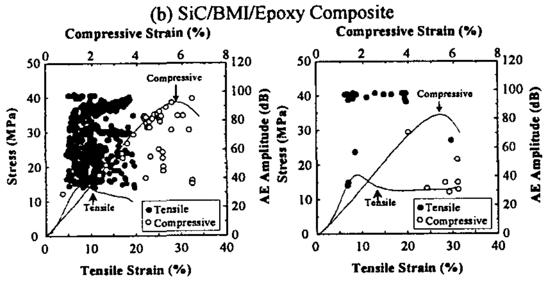

(c) GF/BMI/Epoxy Composite

Fig. 7. AE Amplitude with Stress-Strain Curves for Curing Stages under Tensile/Compressive Tests: (a) CF/BMI/Epoxy Composites, (b) SiC/BMI/Epoxy Composites, (c) GF/BMI/Epoxy Composites.

AE amplitude of BMI matrix fracture occurred at higher value than fiber fracture signal. In case of 2-stage, the amplitude of 3 fibers occurred at certain high amplitudes of fibers, whereas 3 fiber signals decreased at 3-stage. It could be considered that aromatic-hetero-cyclic BMI structure by complete cure might play a role of reduction of the amplitude of fiber failure.

Figure 8 and 9 show AE waveforms and their FFT in carbon fiber/BMI/Epoxy composites under tensile and compressive tests, respectively. In case of tensile fragmentation test, waveform from the fiber breakage and BMI inner matrix fracture and epoxy outer matrix cracking were observed. The maximum AE voltages coming from waveform of BMI matrix fracture were much lager than the carbon fiber breakage. In compressive test the waveform of BMI matrix fracture did not occur, whereas waveform of carbon fiber and epoxy matrix only occurred. The maximum AE voltages coming from the carbon fiber break waveform under compressive test were much small than those under compressive test. It is because of the difference of failure energies between tensile and compressive loading.

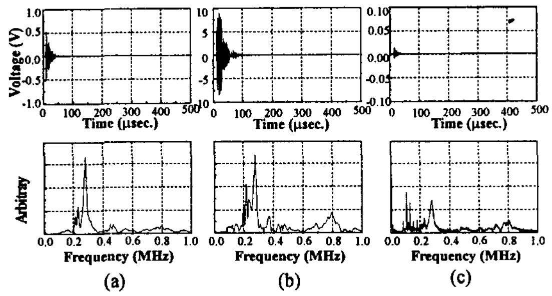

Fig. 8. AE Waveforms and their FFT in Carbon Fiber/BMI/Epoxy Composites: (a) Carbon Fiber, (b) BMI Matrix Fracture, (c) Epoxy Matrix Cracking Under Tensile Tests.

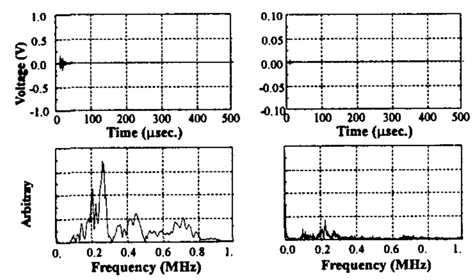

Fig. 9. AE Waveforms and their FFT in Carbon Fiber/BMI/Epoxy Composites: (a) Carbon Fiber, (b) Epoxy Matrix Cracking Under Compressive Tests.

4. CONCLUSIONS

Using tensile/compressive fragmentation tests, IFSS was improved by increasing curing temperature. Failure modes at 3-stage curing cycling showed a sharp fracture due to the aromatic-hetero-cyclic structure of the matrix, whereas 2-stage curing cycling appeared dully failure. In compressive test for fiber reinforced BMI composites, diagonal slippages of fiber appeared due to transverse tensile stress characteristic at the interface. AE test monitored the fracture signals of microfailure sources, such as fiber break, matrix cracking, especially diagonal slippage in the broken fiber ends. AE events were separated well under tensile testing, whereas AE distributions were rather closely overlapped under compressive test. For tensile test, BMI matrix fracture occurred at higher value than carbon, SiC and glass fiber breaks. For compressive test, BMI matrix fracture did not occur, whereas all fiber fracture appears the diagonal slippage in broken fiber. Case of SiC and glass fiber composites, under both tensile/compressive tests, fiber fracture partially appeared due to fiber's high failure strain. The maximum AE voltage for the waveform of BMI matrix fractures under tensile tests exhibited much larger than fiber breakage, due to degree of curing completeness.

ACKNOWLEDGEMENT This study was supported financially by KOSEF through the Research Center for Aircraft Parts Technology (ReCAPT), Gyeongsang National University.

REFERENCES

1) J. M. Park, W. G. Shin, and D. J. Yoon, "Interfacial aspects of two basalt and SiC fiber reinforced epoxy composites using fragmentation technique and acoustic emission", *Compo. Sci. Technol.*, Vol. 59, 1999, pp. 355-370.

2) S. I. Lee, J. M. Park, D. W. Shin, and D. J. Yoon, "Interfacial properties of glass fiber/brittle-ductile dual-matrix composites using micromechanical technique and acoustic emission", *Polymer Compos.*, Vol. 20. 1999, pp. 19-28.

3) X. F. Yang and K. M. Knovels, "The one-dimensional Car packing problem and its application to the distribution of spacing between matrix cracks in unidirectional fiber-reinforced brittle materials", *J. Am. Ceram. Soc.*, Vol.75, 1992, pp. 141-147

4) J. R. Wood, H. D. Wagner, and G. Marom, "The compressive fragmentation phenomenon: using microcomposites to evaluate thermal stress, single fibre compressive strengths, Weibull parameters and interfacial shear strength", *Proc. R. Soc. Lond. A*, 452, 1996, pp. 235-252.

5) K. Gutfreünd, L. J. Broutman and E. H. Jaffe Interfacial investigations of boron fiber-reinforced plastic", *10th SAMPE Sympo.*, 1968

6) C. Ageorges, K. Friedrich, T. Schüller and B. Lauke, "Single-fiber Broutman test: fiber-matrix interface transverse debonding", *Composites:Part A*, Vol. 30, 1999, pp. 1423-1434.

7) J. M. Park, Y. M. Kim, K. W. Kim, and D. J. Yoon, "Interfacial aspects of electrodeposited carbon fiber-reinforced epoxy composites using monomeric and polymeric coupling agents", *J. Collo. Interf. Sci.*, 2000, (in press).